1 June 1998

ELSEVIER

Optics Communications 151 (1998) 241–246

OPTICS COMMUNICATIONS

Precise measurements and analysis of linear and nonlinear optical properties of glass materials near 1.5 μm

L. Canioni *, M.-O. Martin, B. Bousquet, L. Sarger

CPMOH, Université Bordeaux I, 351 cours de la Libération, 33405 Talence Cedex, France

Received 3 December 1997; revised 2 February 1998; accepted 4 February 1998

Abstract

We adapted a time resolved Mach–Zehnder interferometric technique using a synchronously pumped optical parametric oscillator to measure accurate and absolute nonlinear χ^3 in the IR telecommunications domain. Results have been obtained for various metal oxide glasses. Taking into account measurements done at different wavelengths using the same set-up, dispersion of electronic nonlinearity has been studied. Thermal properties have also been measured and very low absorption coefficients of these materials have been analyzed. © 1998 Elsevier Science B.V. All rights reserved.

1. Introduction

Accurate measurement of nonlinear third order susceptibilities has long been a bottleneck, not only at a fundamental level for the modeling of the electromagnetic interaction, but also for the development and optimization of nonlinear materials for real world applications. For example, the wide variety of available techniques can lead to puzzling discrepancy between measured values for the very same material, mostly related to underestimated error bars. Measurement on guided devices such as wave-guides, although precise in the near infrared spectral region (1.3 or 1.5 μm communication wavelengths), are not useful for material investigation. Bulk measurements are essential to account precisely for self phase modulation in the system designs. Moreover, the origin and dispersion of the electronic third order nonlinearities are of great concern to understand the sample spectroscopy as well as to control the ultimate developments for multi-wavelength communication systems. As the electronic response is expected to be very fast, a time resolved absolute measurement in the 100 fs range will give useful data to select materials for ultrafast photonic devices. Usually, the knowledge of the fast and accumulated nonlinear response mainly due to the one and two photon absorption is sufficient to fully characterize a bulk sample [1]. Attempts to understand the mechanism of the nonlinearity in terms of resonant/non-resonant contributions [2] require systematic precise measurements at various wavelengths. As glasses have shown advantages compared to semiconductors, doped systems and organic materials in terms of adaptability and compatibility with wave-guide fabrication procedure, several research groups have studied extensively non-resonant materials as sulphide or titanium oxide glasses [3]. Up to now, although new accurate measurements are readily available [4,5], the lack of a stable laser source has precluded the near infrared spectral region and we report in this Letter the extension of the time resolved interferometric technique using the new synchronously pumped optical parametric oscillator at 1.5 μm. Comparison with data obtained near 0.8 μm on various promising nonlinear oxide glasses will also be presented. Due to the high repetition rate of the laser source, even a very low absorption coefficient can be measured in the same set-up using the accumulated signal. Results for commercial glass will be presented.

* E-mail: canioni@renne.cpmoh.u-bordeaux.fr

0030-4018/98/$19.00 © 1998 Elsevier Science B.V. All rights reserved.
PII S0030-4018(98)00071-6

2. Experimental set-up

Fig. 1 shows the apparatus similar to the one designed for the near infrared [6]. Basically, a Mach–Zehnder interferometer compares the two beams (probe and reference) in amplitude and phase. The sample is located in the probe arm and interacts with the stronger collinear pump beam. The laser used in this set-up is an OPO pumped by a TiSa oscillator (an OPAL and Tsunami from Spectra Physics), which delivers linearly polarized pulses of 150 fs (HWHM) at around 1.5 μm with peak power of 10 kW. It enables us to measure with the same set-up ultra fast and slow nonlinearities by carefully analyzing the nonlinear behaviour at different time delays τ between the pump and the probe. First, without the pump beam, the interference between reference and probe beam is adjusted via delay DII and the fringe contrast is optimized with the help of two adjustable frustrated total internal reflectors to take into account all the differential losses between the two arm intensities. While keeping a perfect overlap between the two beams, an afocal in the probe arm provides a convenient beam waist in the sample and controls the phase front to obtain a far field interference pattern free of any fringes. The sample is located at the beam waist (size $W_0 = 10$ μm) at the focus of a 4 cm focal lens at $\lambda = 1500$ nm. The signal from the two photodiodes $PD_{1,2}$ connected in opposition, is used to lock the interferometer via a high voltage amplifier and a piezoelectric transducer PZT1 and measure the pump induced phase shift in the sample. The calibration factor was easily measured by recording the whole interference fringe as the path difference is varied using PZT1. An electronic servo bandwidth of $f_c = 1.5$ kHz was sufficient to reduce mechanical instabilities and index fluctuations down to a phase noise of 0.1 mrad. In order to improve the signal to noise ratio, the pump beam is electro-optically modulated in amplitude at frequency higher than f_c. The resulting modulation of the signal is recorded using a spectrum analyzer (Tektronix 2622) and the evolution of the amplitude and phase of the relevant Fourier component recorded as a function of the delay τ DI gives the dynamics of the optical nonlinear processes.

3. Signal analysis and results

Absolute measurement in this spectral domain using a synchronously pumped OPO requires special care due to its lower peak power and overall stability as compared to a TiSa KLM source. Analysis of the beam propagation inside the whole set-up, measurement of beam sizes, average of the power spectrum of the laser and interferometric and two photon intensity autocorrelations (in a silicon diode [7]) of pump and probe pulses at the sample position give all the relevant parameters needed for a highly accurate interpretation of the experimental data. All these parameters are checked periodically during acquisition.

As expected for a purely non-resonant glass sample, the signal arises from an instantaneous electronic process and the typical response is displayed in Fig. 2. The collinear configuration leads to a signal whose average is due to the cross correlation between pump and probe fields and oscillations are due to third order coupling processes. The

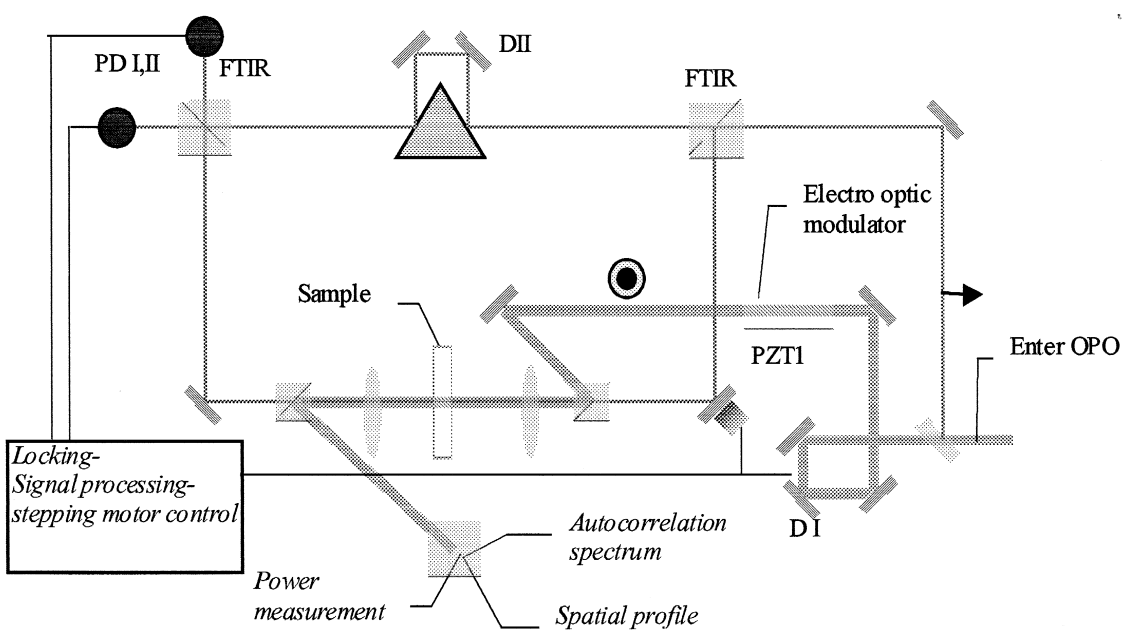

Fig. 1. Experimental set-up.

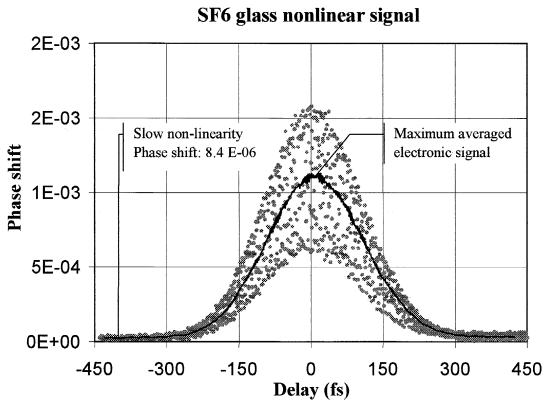

Fig. 2. Interferometric time resolved nonlinear signal.

maximum average phase shift, free from any coherent contributions is related to the nonlinear index by:

$$n_2 = \frac{\Delta\varphi\,\lambda\tau_p^2\sqrt{2}}{P_{\text{pump}} \times 4\pi \arctan\left(l\lambda/2\pi W_0^2\right)}. \quad (1)$$

In this orthogonal pump probe polarization scheme the determination of χ_{xxyy} will be sufficient to characterize the nonlinear response since the fourth rank tensor is totally symmetric among its indices (i.e. $3\chi_{xxyy} = 3\chi_{xyyx} = \chi_{xxxx}$) for isotropic materials.

The above linear relationship can be used to extract the sign and as every parameter in this expression is carefully controlled, an absolute value of the instantaneous nonlinear refractive index can be computed. The accuracy of all optical parameters limits the precision of our measurements to roughly 10%. The sensitivity of this interferometer is around 10^{-20} m^2/W mainly due to the moderate peak power of the OPO.

Table 1 displays some results for commercial materials as well as some experimental glasses as new materials for nonlinear photonic applications. These were proposed and developed at the chemistry departments either in Bordeaux (ICMCB) or in Limoges (LMCTS).

As an example, the two first measurements in silicate glasses display, although in good agreement with previously published values [8], a large dependence on glass composition (mainly OH content).

All experimental glasses have large nonlinearity correlated to the high hyperpolarizability of (Te, Ti, and Nb) ions as part of the glass structure. Some of them, especially those with tellurium [9], are very promising and attempts are being made to develop guiding structures. Ab initio and semi-empirical calculations have been performed in order to analyze the origin of the nonlinearity. They show a strong relationship between local structure and hyperpolarizability [10].

3.1. Nonlinear dispersion

Using the same technique, measurements have been also performed around 850 nm and the dispersion of the nonlinearity can be analyzed. As an example we will take tellurium–niobium glasses because they present promising performances for all optical devices. The relationship between the nonlinear index n_2, the linear index and its dispersion in terms of Abbe number (BGO theory) has been acknowledged for long [11]. Many transparent materials have been successfully screened using this approach. As this theory only predicts the low frequency behaviour of the nonlinearity, no differential dispersion can be found between the linear and nonlinear index. Recently, a new method has been proposed [2] to analyze experimental data

Table 1
Nonlinear index results

Material	Group index	Nonlinear index (m^2/W)	χ^3_{xxxx} (V^2/m^2)
Suprasil	1.422 ± 0.03	$(0.25 \pm 0.2) \times 10^{-19}$	0.089×10^{-21}
Herasil	1.467 ± 0.01	$(0.121 \pm 0.090) \times 10^{-19}$	0.046×10^{-21}
PbF2 (crystal)	1.740 ± 0.01	$(1.93 \pm 0.42) \times 10^{-19}$	1.03×10^{-21}
SF6	1.788 ± 0.01	$(2.15 \pm 0.23) \times 10^{-19}$	1.20×10^{-21}
92 TeO_2–8 Nb_2O_5	2.131 ± 0.03	$(6.12 \pm 0.77) \times 10^{-19}$	4.91×10^{-21}
90 TeO_2–10 Nb_2O_5	2.144 ± 0.03	$(6.93 \pm 0.72) \times 10^{-19}$	5.63×10^{-21}
85 TeO_2–15 Nb_2O_5	2.145 ± 0.05	$(6.41 \pm 0.93) \times 10^{-19}$	5.21×10^{-21}
80 TeO_2–20 Nb_2O_5	2.166 ± 0.05	$(5.94 \pm 0.81) \times 10^{-19}$	4.93×10^{-21}
70 TeO_2–30 Tl_2O	2.125 ± 0.02	$(8.6 \pm 1.0) \times 10^{-19}$	6.87×10^{-21}
65 TeO_2–35 Tl_2O	2.094 ± 0.02	$(8.9 \pm 1.0) \times 10^{-19}$	6.90×10^{-21}
74 TeO_2–24 Tl_2O–2 Bi_2O_3	2.156 ± 0.07	$(9.1 \pm 1.7) \times 10^{-19}$	7.48×10^{-21}
90 TeO_2–10 Al_2O_5	2.003 ± 0.06	$(5.38 \pm 1.19) \times 10^{-19}$	3.81×10^{-21}
Borophosphate–30 Nb_2O_5 [16]	1.772 ± 0.03	$(2.06 \pm 0.25) \times 10^{-19}$	1.14×10^{-21}
Borophosphate–30 TiO_2 [17]	1.615 ± 0.03	$(1.33 \pm 0.26) \times 10^{-19}$	0.61×10^{-21}
86.5 $CaPO_3$–13.5 Nb_2O_5	1.608 ± 0.05	$(0.18 \pm 0.83) \times 10^{-19}$	0.08×10^{-21}

taking into account mainly two-photon absorption. These authors used a two-band model to calculate the nonlinear absorption. They derived the corresponding nonlinear refractive index using a Kramers–Kronig transformation. They have predicted an especially good scaling in a wealth of different materials – semiconductors and insulators – consistent with a universal dispersion curve. As the only parameters needed are the band gap E_g the excitation wavelengths and the linear indices we have scaled our experimental results [12] around $\lambda_i = 850$ nm and 1.5 μm following the expression:

$$R_{exp} = \frac{n_2(\lambda_1)}{n_2(\lambda_2)} \frac{n_0(\lambda_2)}{n_0(\lambda_1)} = \frac{G_2(X_1)}{G_2(X_2)}, \quad (2)$$

where $G_2(X)$ is the dispersion function of a two photon process with argument $X_i = h\omega_i/E_g$,

$$G_2(X) = \frac{1}{2X^6}\left[-\tfrac{3}{8}X^2(1-X)^{-1/2} + 3X(1-X)^{1/2} - 2(1-X)^{3/2} + 2\theta(1-2X)^{5/2}\right], \quad (3)$$

where θ is the step function. At the experimental wavelengths, the calculated dispersion function ratio is:

$$R_{theory} = 2.2(\pm 0.1),$$

with an accuracy only given by spectral uncertainties in the excitation wavelength and bandgap. The experimental results are displayed in Table 2. This table shows a rather good agreement but outside of our (small) errors bars due to the accuracy of our measurements. As compared to the BGO theory prediction of only $R = 0.20$, these results point out the main two-photon contribution to the imaginary part of $\chi^{(3)}$ as a leading nonlinear process. To fully account for the observed exaltation, one may have to analyze the structural properties of these glasses.

Moreover, as the nonlinear contribution at negative delay between pump and probe pulse in our high repetition rate (76 MHz) experiment arises from accumulated effects, the peak to valley ratio at each wavelength roughly measures the figure of merit of the sample [1]. Although the sample purity will play a significant role in the device switching efficiency, the lower thermal effect associated with the two photon enhancement can be exploited as a powerful tool in material selection.

3.2. Signal analysis for negative delay

In order to observe a negative delay signal (pump before probe), the lifetime of the accumulated third order contributions has to be greater than the recurrence of the oscillator (several ns). Among various phenomena having such long lifetime in glasses, thermal or Raman nonlinearity are the most important. For ultrashort pulses, the spectral width of the laser pulse can excite Raman vibration modes in glasses up to 100 cm^{-1}. To our knowledge this contribution cannot exceed 20% of the electronic nonlinearity for sub 100 fs pulses and for our 150 fs pulses these third order terms are negligible [13] after 13 ns delay. We will here develop a model taking into account only the thermal contribution.

3.2.1. The thermal effect

Under laser pumping, the temperature increase (ΔT) in the sample arises from the residual absorption coefficient of the glass (α). The corresponding refractive index change is given by:

$$\Delta n = \frac{\partial n}{\partial T}\Delta T. \quad (4)$$

As this thermal effect is non-local, the value of $\Delta n(r_0)$ is not directly related to the absorption in the glass at r_0, but can be recovered via the heat equation solution with a heating source Q:

$$\frac{\partial}{\partial t}(\Delta T) + D_{th}\nabla^2(\Delta T) = Q(r,t,z). \quad (5)$$

In our case Q is proportional to the fundamental Gaussian mode beam waist W_0 of the pump beam (intensity I_{pump}, power P_{pump}), D_{th} is the thermal diffusivity coefficient (mm^2/s).

The analytical solution of this equation is not straightforward as the heating source has coupled variables (z,r), but if the sample length l is of the order of the pump beam confocal parameter, Q is almost z independent,

$$Q(r,z,t) \approx Q(r,t). \quad (6)$$

Under this condition, Dabby and Boyko [14] have shown that the solution can be split in two parts:

$$\Delta T(r,z) = \Delta T^{(1)}(r)\Delta T^{(2)}(z). \quad (7)$$

For a finite medium where the boundary condition $\Delta T(r,z) = 0$ applies, the longitudinal temperature profile

Table 2
Experimental dispersion function ratio

Material	Nonlinear index (m^2/W) at $\lambda = 850$ nm	R_{exp}
90 TeO_2–10 Nb_2O_5	$(23.3 \pm 2.3) \times 10^{-19}$	3.29 ± 0.6
85 TeO_2–15 Nb_2O_5	$(21.7 \pm 2) \times 10^{-19}$	3.40 ± 0.6
80 TeO_2–20 Nb_2O_5	$(21.6 \pm 2.1) \times 10^{-19}$	3.58 ± 0.6

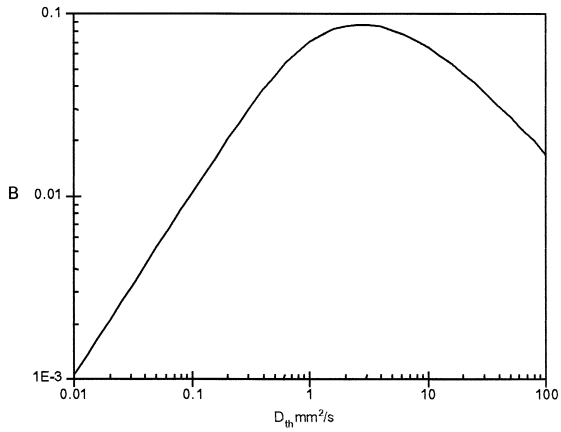

Fig. 3. Variation of B versus D_{th} in log–log scale.

$\Delta T^{(2)}(z)$ appears as a quasi-gate function for very low absorption and a beam waist much smaller than the sample width. Thus, as the longitudinal profile is almost z independent, the analysis can be done in only two dimensions.

3.2.1.1. Solution of heat equation. The steady state solution of Eq. (5) is very sensitive to the boundary condition, because the sample shape will determine the temperature maximum and gradient. Although some solutions have been found for a simple cylindrical shape [15], usually, it is very difficult to interpret the experimental results.

In our case our modulated experiment is not adapted to a DC analysis, but rather the source term can be conveniently expressed as:

$$Q(r,t) = \alpha I_{\mathrm{pump}}(r)\left[\tfrac{1}{2} + \tfrac{1}{2}\sin(2\pi Ft)\right]. \tag{8}$$

The first part of this expression is time independent and accounts for the permanent heating in the sample (steady state regime). The second part is the modulated AC source leading to no net average heating, instead the temperature at a particular time could be hotter or colder than the surrounding mean temperature. As is well known to a meteorologist and wine keeper, the modulated temperature is not sensitive to the sample shape.

Eq. (5) will then be easily solved in the Fourier space (q,r) using the Hankel transformation with the boundary condition. The permanent solution is given by:

$$\Delta T(q,t) = \alpha P_{\mathrm{pump}} A \frac{\exp\left(-q^2 W_0^2/8\right)}{D_{\mathrm{th}}^2 q^4 + (2\pi F)^2}\left[D_{\mathrm{th}} q^2 \sin(2\pi Ft) - (2\pi F)\cos(2\pi Ft)\right], \tag{9}$$

where A stands for the thermodynamic properties of the glass (density ρ and heat capacity c_{p})

$$A = 1/\rho c_{\mathrm{p}}. \tag{10}$$

We used the Perseval theorem to compute the experimental phase shift $\Delta\varphi_{\mathrm{th}}(t)$:

$$\Delta\varphi_{\mathrm{th}}(t) = \frac{2\pi l}{\lambda}\frac{\partial n}{\partial t}\frac{\int_0^\infty I_{\mathrm{probe}}(q)\Delta T^*(q,t)2\pi q\,\mathrm{d}q}{\int_0^\infty E_{\mathrm{probe}}(q)E^*_{\mathrm{probe}}(q,)2\pi q\,\mathrm{d}q}. \tag{11}$$

A numerical estimation of this expression shows that the cosine contribution is one order of magnitude lower than the sine one. This is experimentally confirmed using our vectorial spectrum analyzer that measures separately both terms.

Carrying out the integrations one gets:

$$\Delta\varphi_{\mathrm{th}} = \frac{l}{\lambda}\frac{1}{\rho c_{\mathrm{p}}}\frac{\partial n}{\partial T}\alpha\frac{P_{\mathrm{pump}}}{2}B(D_{\mathrm{th}},W_0,F), \tag{12}$$

where the thermal diffusivity appears only in the B function:

$$B(D_{\mathrm{th}},F,W_0) = \int_0^\infty \frac{D_{\mathrm{th}} q^3 \exp\left(-q^2 W_0^2/4\right)}{D_{\mathrm{th}}^2 q^4 + (2\pi F)^2}\,\mathrm{d}q. \tag{13}$$

A plot of this function is presented in Fig. 3

3.2.1.2. Results. To check the validity of this approach we analyze a commercial glass from Schott SF6. The result is presented in Table 3. Here, the accuracy is mainly due to the measured thermal phase shift especially small in this case where the glass sample is only few millimetres long and the average laser power is approximately 100 mW. However, for this very low absorption, equivalent to a standard OD = 0.0008, our result clearly reproduces a tabulated value.

Table 3
Theoretical and experimental thermal coefficients for SF6 glass

D_{th} [18] (mm^2/s)	$1/\rho c_{\mathrm{p}}$ $\partial n/\partial T$ [18]	α [a] (cm^{-1})	B Calculated	$\Delta\varphi_{\mathrm{th}}$ Measured	α Experimental (cm^{-1})
0.333	7.29×10^{-3}	4×10^{-3}	0.0327	8.4×10^{-6}	3.6×10^{-3}

[a] Evaluated from Ref. [18].

4. Conclusions

We demonstrate the extension of the time-resolved interferometry to the 1.5 μm telecommunications domain. Precise measurements obtained in the nonlinear and linear regimes on small samples confirm the power of this interferometric approach in the very early stage of material selection for optronic applications. Moreover, such a precise multi-wavelength investigation permits a more fundamental evaluation of the nonlinear processes. Among the various experimental glasses analyzed in this study some of them, especially tellurium oxides, appeared to be very promising for all optical nonlinear devices and will be integrated as guided structures.

Acknowledgements

Acknowledgements to the chemical staff (G. Leflem, ICMCB University Bordeaux I and P. Toma, LMCTS University Limoges) for the sample preparation and many helpful discussions.

References

[1] S.R. Fryberg, P. Smith, IEEE J. Quantum Electron. QE 23 (1987) 2089.
[2] M. Sheik-Bahae, D.J. Hagan, E.W. Van Stryland, Phys. Rev. Lett. 65 (1990) 96.
[3] I. Kang, T.D. Krauss, F.W. Wise, B.G. Aithken, N.F. Borelli, J. Opt. Soc. Am. B 12 (1995) 2053.
[4] I. Kang, T. Krauss, F. Wise, Optics Lett. 22 (1997) 14.
[5] L. Canioni, L. Sarger, P. Segonds, A. Ducasse, C. Duchesne, E. Fargin, R. Olazcuaga, G. Le Flem, Solid State Commun. 84 (1992) 11.
[6] L. Sarger, P. Segonds, L. Canioni, F. Adamietz, A. Ducasse, C. Duchesne, E. Fargin, R. Olazcuaga, G. Le Flem, J. Opt. Soc. Am. B 11 (1994) 000.
[7] D.T. Reid, M. Padgett, C. McGowan, W.E. Sleat, W. Sibbett, Optics Lett. 22 (1997) 4.
[8] A. Boskovic, S.V. Chernikov, J.R. Taylor, Optics Lett. 21 (1996) 24.
[9] A. Berthereau, Ph.D. Thesis, University Bordeaux I, 1995.
[10] S. Le Boiteux, P. Segonds, L. Canioni, L. Sarger, T. Cardinal, C. Duchesne, E. Fargin, G. Le Flem, J. Appl. Phys. 1997.
[11] N.L. Boling, A.J. Glass, A. Owyoung, IEEE. J. Quantum Electron. 14 (1978) 601.
[12] A. Berthereau, Y. Le Luyer, R. Olazcuaga, G. Le Flem, M. Couzi, L. Canioni, P. Segonds, L. Sarger, A. Ducasse, Mater. Res. Bull. 29 (9) (1994) .
[13] R. Hellwarth, J. Cherlow, T.-T. Yang, Phys. Rev. B 11 (1975) 2.
[14] F. Dabby, R. Boyko, IEEE J. Quantum Electron. 5 (1965) 520.
[15] Gordon, Leite, J. Appl. Phys. 36 (1965) 3.
[16] T. Cardinal, E. Fargin, G. Le Flem, L. Canioni, P. Segonds, L. Sarger, A. Ducasse, F. Adamietz, Eur. J. Solid State Inorg. Chem. 3b (1996) 597.
[17] T. Cardinal, E. Fargin, G. Le Flem, L. Canioni, P. Segonds, L. Sarger, F. Adamietz, A. Ducasse, Eur. J. Solid State Inorg. Chem. 31 (1994) 935.
[18] Schott Catalog.